HHS Public Access

Author manuscript

Sci Signal. Author manuscript; available in PMC 2021 November 25.

Published in final edited form as:

Sci Signal. ; 14(684): . doi:10.1126/scisignal.aaz4401.

Phosphorylation of Pal2 by the protein kinases Kin1 and Kin2 modulates *HAC1* mRNA splicing in the unfolded protein response in yeast

Chandrima Ghosh[#1], **Jagadeesh Kumar Uppala**[#1], **Leena Sathe**[1], **Charlotte I. Hammond**[2], **Ashish Anshu**[1], **P Raj Pokkuluri**[3], **Benjamin E. Turk**[4], **Madhusudan Dey**[1,*]

[1]Department of Biological Sciences, University of Wisconsin-Milwaukee, Milwaukee, WI 53211

[2]Department of Biological Sciences, Quinnipiac University, Hamden, CT, 06518

[3]Bioscience Division, Argonne National Laboratory, Lemont, IL 60439

[4]Department of Pharmacology, Yale University School of Medicine, New Haven, CT 06520

[#] These authors contributed equally to this work.

Abstract

During cellular stress in the budding yeast *Saccharomyces cerevisiae*, an endoplasmic reticulum (ER)-resident dual kinase and RNase Ire1 splices an intron from *HAC1* mRNA in the cytosol, thereby releasing its translational block. Hac1 protein then activates an adaptive cellular stress response called the unfolded protein response (UPR) that maintains ER homeostasis. The polarity-inducing protein kinases Kin1 and Kin2 contribute to *HAC1* mRNA processing. Here, we showed that an RNA-protein complex that included the endocytic proteins Pal1 and Pal2 mediated *HAC1* mRNA splicing downstream of Kin1 and Kin2. We found that Pal1 and Pal2 bound to the 3'-untranslated region (3'-UTR) of *HAC1* mRNA, and a yeast strain lacking both Pal1 and Pal2 was deficient in *HAC1* mRNA processing. We also showed that Kin1 and Kin2 directly phosphorylated Pal2, and that a non-phosphorylatable Pal2 mutant could not rescue the UPR defect in a *pal1Δ pal2Δ* strain. Thus, our work uncovers a Kin1/2-Pal2 signaling pathway that coordinates *HAC1* mRNA processing and ER homeostasis.

INTRODUCTION

Almost one third of cellular proteins fold and mature inside the endoplasmic reticulum (ER). Cellular stresses that cause accumulation of misfolded proteins within the ER trigger a

[*]Corresponding author: Madhusudan Dey, Department of Biological Sciences, University of Wisconsin-Milwaukee, 3209 N Maryland Ave, Milwaukee, WI-53211, Phone: 414-229-4309, deym@uwm.edu.

AUTHOR CONTRIBUTIONS:

M.D. and B. E. T. designed the experiments. C.G., L.S., J.U., A. A. C.I.H performed experiments and analyzed results. M.D. and B.E.T. wrote the manuscript. All authors read and approved the final manuscript.

COMPETING INTERESTS:

The authors declare that they have no competing interests.

DATA AND MATERIALS AVAILABILITY: The mass spectrometry data have been deposited to MassIVE repository (reference number MSV000087142, ftp://massive.ucsd.edu/MSV000087142/). All other data needed to evaluate the conclusions in the paper are present in the paper or the Supplementary Materials.

network of intracellular signaling pathways collectively known as the unfolded protein response (UPR) (1–4). A key molecular event in the UPR signaling pathway is co-localization of *HAC1* mRNA in budding yeast (5–7) or *XBP1* in metazoans (8–10) with the ER-resident protein kinase and endonuclease Ire1 (11–13). Ire1 subsequently cleaves an intervening sequence from *HAC1* mRNA in yeast and *XBP1* mRNA in mammals. The spliced form of *HAC1/XBP1* mRNA encodes a transcription factor that induces the expression of numerous proteins, including ER-resident chaperones, to enhance the protein folding capacity of the cell. Although delivery of the unspliced *HAC1/XBP1* mRNA to Ire1 is a critical step in propagating the UPR, mechanisms that drive their co-localization are still unknown. We identified the closely related protein kinases Kin1 and Kin2 as high copy suppressors of a mutation in the cis-acting 3'-bipartite element (3'-BE) located at the 3'-untranslated region (3'-UTR) of the *HAC1* mRNA, and showed that both splicing and translation of *HAC1* mRNA are impaired in strains lacking both Kin1 and Kin2 (14). Thus, we speculate that Kin kinases likely promotes the formation of a ribonucleoprotein (RNP) complex on the 3'-BE of *HAC1* mRNA, which facilitates co-localization of *HAC1* mRNA with Ire1.

Kin1 and Kin2 belong to a subfamily of the AMP-activated kinase-related kinases (AMPKRs) that regulate cell polarity in other species (15). Other members of this subfamily are Kin1 in fission yeast (*Schizosaccharomyces pombe)*(16), Kin10 and its isoforms in plants (*Arabidopsis thaliana)* (17), Par-1 in the worm (*Caenorhabditis elegans)* (18), and MARKs (microtubule affinity-regulating kinases) in mammals (19). These polarity-inducing kinases share extensive amino acid sequence similarity and contain a highly conserved N-terminal protein kinase domain (KD) and a C-terminal kinase associated domain 1 (KA1) separated by a long spacer of unknown function. Some of these kinases also contain a ubiquitin-associated (UBA)-like domain immediately after their kinase domain. Several lines of evidence indicate that intra-molecular interaction between the KD and KA1 domains keeps the kinases inactive under normal conditions. In response to extracellular and intracellular cues, the KD is activated, which promotes cell polarity and tissue morphogenesis through phosphorylation of various target proteins (20). Additionally, Kin isoforms in budding yeast may play a role in cellular exocytosis (21,22). However, it remains unclear how these kinases orchestrate cell polarity and/or UPR.

The Kin/Par-1/MARK family of kinases phosphorylate various substrates. In the fission yeast *S. pombe*, Kin1 phosphorylates three polarity proteins (pal1, mod5, and tea4) at multiple sites (23). In *C. elegans*, Par-1 phosphorylates Mex5, Mex6 and LIN-5 (24). Human MARK isoforms phosphorylate KXGS motifs in the repeat domain of Tau which stabilizes microtubules (25). Despite these advances in our understanding of these substrates, the physiological importance of substrate phosphorylation in cell polarity or tissue morphogenesis are not clearly defined.

In our search for the core 3'BE-RNP that contributes to the targeting of *HAC1* mRNA to the ER stress site, we identified two proteins, Pal2 and its paralog Pal1. We found that a yeast strain lacking both Pal1 and Pal2 was deficient in *HAC1* mRNA splicing, suggesting that Pal proteins regulated *HAC1* mRNA processing. The similarity of this phenotype to that of cells lacking Kin1 and Kin2 (14) led us to speculate that they act in a common pathway, and we

showed that Pal2 is a direct substrate of Kin kinases *in vitro* and *in vivo* (26). Overall, this work identifies a regulator of *HAC1* mRNA splicing in the cytosol and a Kin2-Pal2 signaling pathway that contributes to *HAC1* mRNA processing and ER homeostasis.

RESULTS

Analysis of the 3'-BE-binding proteomes identifies Pal2 as a putative *HAC1* mRNA binding protein.

The *HAC1* mRNA 3'-UTR contains a cis-acting 3'-BE at nucleotides C_{1134} to A_{1192} (where adenine of the AUG codon is +1) (Figs. 1A and 1B) with two consensus elements (5'-$G_{1143}GCGC_{1147}$-3' and 5'-$G_{1180}CGAC_{1184}$-3')(7). This *cis*-acting 3'-BE promotes co-localization of the translationally repressed *HAC1* mRNA with Ire1 when cells are under ER stress. We speculated that recruitment of *HAC1* to Ire1 might involve a set of proteins that interact with the 3'-BE, prompting us to search for 3'-BE-associated proteins. We prepared a construct in which the 3'-BE (Figs. 1A and 1B, nucleotides C_{1134} to G_{1192}) was conjugated to a 43-nucleotide RNA aptamer mimicking biotin (27) [abbreviated here as the RMB (RNA mimic of biotin)] and placed under control of the constitutive yeast *ADH1* promoter. As a control, we also prepared a 5'-RD (RNA duplex)-RMB construct to express an RNA product composed of a 24-nucleotide 5'-UTR sequence (Figs. 1A and 1B, U_{-19} to U_{-42}), a 21-nucleotide intronic sequence (U_{763} to A_{783}) and the 43-nucleotide RMB. We expected that the 5'-RD-RMB mini RNA would fold and mimic the 5'-UTR-intron interaction as we observed in the translationally repressed *HAC1* mRNA (28). Both 3'-BE-RMB and 5'-RD-RMB constructs were introduced separately into a *hac1Δ* strain, and expression of both RNAs was confirmed by RT-PCR (Fig 1C). Next, we grew yeast cells in the presence of 4-thiouridine (4sU) to label the uracil residues of these mini RNAs with thiol groups. The 4sU-labeled RNA and associated proteins were photo-crosslinked by UV-irradiation as described previously (29). RMB-conjugated RNAs were immobilized on streptavidin-agarose, and bound proteins were eluted and subjected to LC tandem mass spectrometry (LC-MS/MS) (Fig 1D). Multiple common mRNA binding proteins (such as small and large ribosomal subunit associated proteins and general translation factors) was identified in each sample (Data File 1). We selected proteins associated uniquely with either the 3'-BE-RMB or the 5'-RD-RMB mini RNA (Table 1) and compared our list of 3'-BE associated proteins with a previously published set of *HAC1* binding proteins (30) and with proteins that had been predicted to be substrates of Kin1/Kin2 based on the presence of an optimal phosphorylation site consensus sequence (26). Only the previously uncharacterized protein Pal2 fits all three criteria.

Both Pal1 and Pal2 proteins contribute to *HAC1* splicing

Pal2 and its paralog Pal1 are reported to regulate clathrin-mediated endocytosis (31), but neither protein has been implicated in the UPR.

To determine whether Pal2 and/or Pal1 were required for activation of ER stress, we generated a *pal1Δ pal2Δ* strain and examined its growth of in the presence or absence of the ER stress-inducing agent tunicamycin (Fig 2A). Although yeast cells lacking both Pal1 and Pal2 grew slightly slower than WT cells on control medium, their growth was substantially

reduced in the presence of tunicamycin (Fig 2A and fig S1A–C). As anticipated, control strains lacking either Ire1 or Hac1 did not grow on tunicamycin-containing medium (Fig 2A). The tunicamycin-induced growth defect of *pal1Δ pal2Δ* cells was exacerbated when cells were grown on media containing galactose, a less preferred carbon source (Fig 2B). Although deletion of *PAL1* alone did not affect growth on tunicamycin medium, single deletion of *PAL2* produced a substantial growth defect, albeit less severe than with that produced by combined deletion of both genes (Fig 2B). We used galactose-based medium in subsequent studies because it allowed us to use low tunicamycin concentrations that were less likely to cause non-specific toxicity.

The reduced growth on the tunicamycin-containing medium could be due to a defect in *HAC1* mRNA splicing, Hac1 protein expression, or both. Only unspliced *HAC1* mRNA ($HAC1^{u}$) was observed in WT cells grown in the absence of tunicamycin, whereas both unspliced and spliced ($HAC1^{s}$) *HAC1* mRNAs were observed in the presence of tunicamycin (Fig 2C). As anticipated, tunicamycin robustly induced Hac1 protein expression in WT cells (Fig 2D). The *pal1Δ pal2Δ* strain showed significantly reduced splicing of *HAC1* mRNA (Fig 2C) and Hac1 protein expression from the spliced mRNA (>50%) (Fig 2D). As we reported earlier, *HAC1* mRNA splicing and protein expression was reduced to a similar extent in *kin1Δ kin2Δ* cells (14). Consistent with the tunicamyin-induced decrease in growth (Fig 2B), we observed that Hac1 protein expression was reduced (40%) in the *pal2Δ* strain but not in the *pal1Δ* strain (Fig 2D, compare lanes 5 and 7). These data suggest that Pal1 and Pal2 contribute to *HAC1* mRNA splicing and/or translation, with Pal2 having the predominant role.

To further confirm that Pal1 and Pal2 proteins contribute to the UPR, we examined trans-activation of an *UPRE*-driven *LacZ* reporter in the *pal1Δ pal2Δ* strain (32). In WT cells, *UPRE*-driven *lacZ* expression was elevated about 6-fold when cells were treated with the ER stressor DTT, an effect that was reduced in the *pal1Δ pal2Δ* and *kin1Δ kin2Δ* strains (Fig 3A). To determine whether Pal1 and Pal2 act at the level of *HAC1* mRNA splicing, we examined the growth of strains expressing a plasmid-encoded intron-less *HAC1* construct on tunicamycin-containing medium. As anticipated, the expression of the intron-less *HAC1* gene rescued the growth of an *ire1Δ* strain on tunicamycin medium (Fig 3B). Likewise, intron-less *HAC1* allowed the *pal1Δ pal2Δ* strain to grow in the presence of tunicamycin (Fig 3B), likely because the strain could translate the protein without Ire1-mediated splicing (Fig 3C). These data collectively suggest that Pal1 and Pal2 promote *HAC1* mRNA splicing, likely by targeting the mRNA to the ER stress site.

Truncated Pal proteins bind to the synthetic 3'-BE of *HAC1* mRNA

Atypically for yeast protein coding genes, *S. cerevisiae PAL2* and its orthologs in other species contain an intron of variable length, whereas the paralogous *PAL1* gene does not have any intronic sequence (https://www.yeastgenome.org). Sequence comparison of Pal1 and Pal2 indicate an overall 45% sequence identity, including multiple annotated phosphorylation sites (fig S2). To determine the physiological role of Pal2 in the ER stress response, we generated a Flag-tagged $PAL2^{\Delta intron}$ derivative in which the intron was removed and a Flag-epitope was inserted at its N-terminus (Fig 4A, right panel). Like WT

PAL2, *Flag-PAL2*$^{\Delta intron}$ complemented the *pal1Δ pal2Δ* strain (Fig 4A. row 3). However, Western blot analysis showed a faint protein band from the *PAL2*$^{\Delta intron}$ construct (Fig 4B, lane 3), suggesting that the basal expression of Pal2 in cells was extremely low.

The sequence alignment of Pal1 and Pal2 showed that amino acid residues 165–499 of Pal1 are highly similar to residues 65–366 of Pal2 (fig S2). Moreover, sequence comparison of Pal2 homologs among lower eukaryotes showed that the N-terminal region of Pal2 is highly variable (fig S3). To determine whether the N-terminal residues of Pal2 were functionally redundant, we separately deleted the DNA sequences encoding residues 65 and 135 from the N-terminal end (Fig 4A), generating Flag-tagged *PAL2*$^{\Delta intron}$-ΔN65 *and PAL2*$^{\Delta intron}$-ΔN135 constructs, respectively. We observed that the *PAL2*$^{\Delta intron}$-ΔN65, but not the *PAL2*$^{\Delta intron}$-ΔN135 construct, complemented the *pal1Δ pal2Δ* strain, allowing cells to grow on tunicamycin medium (Fig 4A, rows 4 and 5). Expression of both *PAL2*$^{\Delta intron}$-ΔN65 *and PAL2*$^{\Delta intron}$-ΔN135 was detectable by Western blot (Fig 4B, lanes 4 and 5). These data suggest that the N-terminal 65 residues of Pal2 are dispensable for its function in the UPR, and that *PAL2*$^{\Delta intron}$*-ΔN135* results in a non-functional protein. Like *PAL2*$^{\Delta intron}$*-ΔN65,* we also observed that a truncated Pal1 protein (residues 165–499, referred here to as *PAL1*$^{\Delta N}$) complemented the tunicamycin growth defect of the *pal1Δ pal2Δ* strain (Fig 4C). We used the *PAL2*$^{\Delta intron}$-ΔN65 and *PAL1*$^{\Delta N}$ derivatives for our subsequent studies to determine the physiological function of the respective proteins.

We confirmed the association of Pal1 and Pal2 proteins with *HAC1* mRNA by an electrophoretic mobility shift assay (EMSA) using recombinant Pal1 or Pal2 protein and a fluorescein labeled 3'-BE (Flc-3'-BE). Either Pal1 or Pal2 induced an upward mobility shift of the Flc-3'-BE RNA (Fig 4D), demonstrating that they bound directly to the 3'-BE of *HAC1* mRNA. We also tested the binding of the known *HAC1* mRNA binding protein Ypt1 (30) or a Met-tRNA binding protein eIF2α (33) with Flc-3'-BE. Neither protein caused a mobility shift (Fig 4D), indicating that Flc-3'-BE RNA binds selectively to Pal1 and Pal2, and that Ypt1 presumably interacts with other regions of the *HAC1* mRNA. We also found that co-incubation with unlabeled 3'-BE (synthesized by in vitro transcription) reduced the interaction of Pal2 with Flc-3'-BE (Fig 4E), further confirming that Pal1 and Pal2 specifically bound to the 3'-BE of *HAC1* mRNA.

Kin1 and Kin2 phosphorylate Pal2 in vitro and in vivo at Ser^{222}

In budding yeast, Kin1 and Kin2 have roles in diverse physiological processes, including exocytosis (34) and the ER stress response (14). However, physiological substrate(s) of Kin1 and Kin2 responsible for these roles have not been identified. Positional scanning-oriented peptide library (PSPL) analysis indicated that Kin kinases have a strong preference for sequences containing a conserved N-x-S-x-pT-x-L motif (Fig 5A), where pT represents a phosphorylated threonine at the position +2 of the phosphorylation site (26). Previous analysis of the yeast phosphoproteomics data identified 36 proteins that contained an N-x-S-x-S/T-x-L motif. Out of those 36 proteins, 12 proteins are phosphorylated on the Ser or Thr residue found at position +2, which may "prime" the substrate for subsequent phosphorylation by Kin1 or Kin2. This list includes Pal2, as well as the previously reported Kin1/Kin2 substrate Sec9 (21). To examine whether these candidates might be authentic

Kin1 or Kin2 substrates, we expressed Sec9, Pal2, Kip3, Svl3, Mlf3 and Eap1 proteins in yeast cells from galactose-inducible high-copy plasmids. The expressed proteins were purified as described previously (35) (Fig 5B) and then used in kinase assays (Fig 5C). In addition to Kin1 autophosphorylation, we observed robust phosphorylation of Sec9, Pal2, and Eap1 (Fig 5C). Svl3 and Mlf3 appeared to be phosphorylated to a lesser extent by Kin1, whereas Kip3 had substantial background phosphorylation in the absence of Kin1.

To further confirm that Pal2 is a substrate of Kin, we expressed the Pal2 protein (residues 65–366) in bacteria. Circular dichroism (CD) spectroscopy indicated that recombinant Pal2 was composed of α-helices (10%), antiparallel β-sheet (25%), with the rest is made up of turns and/or irregular structure (Fig. 6A). Thus, it appears that the overall fold of Pal2 protein likely consists of largely irregular structure, which is consistent with the predictions based on its amino acid sequence (figs. S4A and SB).

Next, we performed *in vitro* kinase assays using recombinant Pal2 as substrate and Kin2 or PKR as kinase. PKR specifically phosphorylates the translation initiation factor eIF2α (eIF2α) to regulate cellular translation (36). As expected, we found that eIF2α was readily phosphorylated by PKR, but not by Kin2 (Fig 6B). In contrast, Pal2 was readily phosphorylated by Kin2, but not by PKR. These results suggest that Pal2 is a specific substrate of Kin2. To map specific sites of phosphorylation, Kin2-phosphorylated Pal2 was subjected to LC-MS/MS analysis (figs. S5A, S5B and S6). We identified a major phosphorylated tryptic peptide (ANSSTTTLDAAIKPNSK) that included the site predicted to be phosphorylated by Kin1/Kin2 (Ser^{222} within the N-x-S-x-T-x-L sequence motif). Of six potential phospho-acceptor residues within this peptide, prior phosphoproteomics studies have found five of them (Ser^{221}, Ser^{222}, Thr^{223}, Thr^{224}, Thr^{225}) to be phosphorylated *in vivo* (37) (fig S5A).

To validate the mass spectrometry results, we performed *in vitro* kinase assays, using a series of Pal2 point mutants (Fig 6C). Combined mutation of four putative phosphorylated residues (Ser^{222}, Thr^{223}, Thr^{224}, Thr^{225}) to alanine (referred to as Pal2-4Ala) reduced the phosphorylation of Pal2 by Kin2 (Fig 6C). By contrast, combined mutation of the three Thr residues (Thr^{223}, Thr^{224}, and Thr^{225}, referred to as Pal2-3Ala) had a more modest effect, whereas mutation of Ser^{222} alone or in combination with Thr^{224} (referred as 2Ala) led to inefficient phosphorylation by Kin2 (Fig 6C and fig S5C). Collectively these data suggest that Ser^{222} is the major site on Pal2 phosphorylated by Kin2 *in vitro*.

We noted that although Pal1 and Pal2 have high sequence similarity, Pal1 lacks the Kin1/Kin2 consensus phosphorylation site sequence, but does have a single threonine residue at position 323, analogous to Thr^{225} of Pal2 (Fig 5A). We also found that the truncated Pal1 protein (residues 165–499) that fully complemented the *pal1Δ pal2Δ* strain was weakly phosphorylated by Kin2 in vitro (Fig. 6D, lane 1). This low level of phosphorylation was not affected by mutation of Thr^{323} to Ala (Fig. 6D, lane 2). These data suggest that unlike Pal2, Pal1 is not a substrate of Kin2.

We next examined whether Kin1 and Kin2 phosphorylated Pal2 *in vivo*. *pal1Δ pal2Δ* and *kin1Δ kin2Δ* strains transformed with plasmids expressing Flag-tagged WT Pal2 protein

were grown under ER stress conditions. Phos-tag SDS gel analysis showed that WT Pal2 was separated into at least three distinct species (Fig 6E, lane 2), suggesting that Pal2 is phosphorylated at multiple sites. Notably, the slowest migrating protein band was absent from samples expressing the Pal2-4Ala mutant, in which two faster migrating protein bands were prominent. A similar pattern was seen when wild-type Pal2 was expressed in *kin1Δ kin2Δ* cells. Together, these data indicate that Pal2 is phosphorylated at one or more sites in the Ser^{222}– Thr^{225} region in a manner dependent on Kin1 and/or Kin2. Along with our observation that Kin2 phosphorylates Ser^{222} *in vitro*, these results suggest that Pal2 is a bona fide *in vivo* substrate of Kin1/Kin2.

Previously, we have shown that phosphorylation of Thr^{281} within the activation loop of Kin2 is important for its activation (38). We purified a functional and truncated form of Flag-tagged Kin2 protein (residues 94–526) from yeast cells (*Sc*Flag-Kin2). We also purified the GST-Kin2 (residues 94–526) and its derivatives GST-Kin2-T281E and GST-Kin2-ΔKI-T281E (ΔKI indicates deletion of the kinase insert region, residues Ala^{136} to Ile^{164}) from *E. coli* (*Ec*GST-Kin2 and *Ec*GST-Kin2-ΔKI-T281E). We performed *in vitro* kinase assays with the recombinant Pal2 protein as a substrate using *Sc*Flag-Kin2, *Ec*GST-Kin2 or *Ec*GST-Kin2-ΔKI-T281E as the kinase. As expected, *Sc*Flag-Kin2 purified from yeast cells and is presumably phosphorylated at Thr^{281} (38) phosphorylated Pal2 (Fig 6F, lane 2). The *Ec*GST-Kin2 protein purified from bacteria was unable to phosphorylate Pal2 (Fig 6F, lane 3). This is most likely because bacterially purified Kin2 protein was not phosphorylated at the activation loop residue Thr^{281}. However, the *Ec*GST-Kin2-ΔKI-T281E protein that contained a phospho-mimetic glutamate in place of Thr^{281} phosphorylated Pal2 (Fig 6F, lane 4). Together, these results suggest that Thr^{281} phosphorylation within the activation loop of Kin2 is required for Pal2 phosphorylation. Moreover, these results further confirm that activation loop phosphorylation of Kin2 occurs in *trans* by another kinase.

Phosphorylation of Pal2 is important for ER stress responses

We next investigated whether Pal2 phosphorylation is important for regulation of the UPR. As shown above, the Flag-$Pal2^{\Delta intron}$-ΔN65 construct encodes a functional protein that complemented the *pal1Δ pal2Δ* double deletion strain (Fig 7A, row 2). In the context of this construct, the S222A mutation did not affect the ability of Pal2 to rescue the tunicamycin growth defect of a *pal1Δ pal2Δ* strain (Fig 7A, row 3). These data suggested that phosphorylation at Ser^{222} alone was dispensable for promoting resistance to tunicamycin. Accordingly, we combined mutations of nearby phosphorylated residues (Thr^{223}, Thr^{224}, and Thr^{225}) with the $Pal2^{\Delta N65}$-S222A mutant. We observed that the *pal1Δ pal2Δ* strain expressing all double (such as S222A, T225A and S222A, T223A) combinations grew on tunicamycin medium (Fig 7A, rows 6 and 7). However, the *pal1Δpal2Δ* cells expressing the $Pal2^{\Delta N65}$-4Ala quadruple mutant ($Pal2^{\Delta N65}$-STTT222–225AAAA) exhibited a slow-growth phenotype compared to its isogenic WT strain and were unable to grow on medium containing tunicamycin (Fig 7A, row 9), which was not because of decreased expression of Pal2 (Fig 7B, lane 9), but rather the low level of Hac1 protein expression (Fig 7C, compare lanes 3 and 4). We also observed that a phosphomimetic $Pal2^{\Delta N65}$-4Glu quadruple mutant ($Pal2^{\Delta N65}$-STTT222–225EEEE) grew on tunicamycin-containing medium (Fig 7A, lane 13), suggesting that the functional impact of mutating these sites to Ala is due to ablating

phosphorylation. It therefore appears that the phosphorylation of Pal2 at Ser^{222}, Thr^{223}, Thr^{224}, and Thr^{225} are important for the tunicamycin resistant phenotype.

To further test whether Pal2 was the sole substrate of Kin2, we introduced the $Pal2^{\Delta N65}$-STTT222–225EEEE mutant in the *kin1Δkin2Δ* double deletion strain, which rendered this strain unable to grow on the tunicamycin-containing medium (Fig 7D, row 4). These data suggested that multiple Kin2 substrates are involved in ER stress resistant. Together, our data suggest that Kin2 phosphorylates Pal2 specifically at Ser^{222}, whereas an unknown kinase(s) might phosphorylate the residues Thr^{223}, Thr^{224}, and/or Thr^{225} (Fig 7E).

The kinase Snf1 does not contribute to ER stress responses

The kinase Snf1 (sucrose non-fermenting 1) potentially engages in priming a substrate (such as Sec9) for subsequent phosphorylation by Kin1/Kin2 (26). To investigate whether Pal2, like Sec9, might be primed by Snf1 phosphorylation, we generated a *kin1Δ kin2Δ snf1Δ* strain. We found that the *kin1Δkin2Δsnf1Δ* strain grew on tunicamycin-containing medium similarly to the *kin1Δkin2Δ* strain (figs. S7A and S7B), in contrast to our expectation that the triple mutant strain would be more sensitive to tunicamycin. We note that the sequence surrounding the Pal2 priming site did not conform to the substrate recognition (L-x-R-x-x-S/T-x-x-x-L) motif of Snf1(39) (Fig 5A). Collectively, these results suggest that Snf1 does not phosphorylates Pal2 under physiological conditions and contribute to the ER stress response. Kinases that phosphorylate Thr^{223}, Thr^{224}, and/or Thr^{225} remain to be identified.

DISCUSSION

In this study, we showed that the endocytic proteins Pal1 and Pal2 contributed to *HAC1* mRNA processing. We also show that Kin1 and Kin2 specifically phosphorylated Pal2, but not its isoform Pal1. Previously, we have shown that Kin1 and Kin2 are required for optimal activation of the UPR (14). Thus, our work reveals a Kin2-Pal2 signaling pathway contributing to *HAC1* mRNA metabolism and ER homeostasis.

Under conditions of ER stress, Ire1 cleaves *HAC1* mRNA at two specific sites (G661 and G913), thus removing an intervening sequence that blocks the initiation of translation (28,40). Cleavage requires co-localization of *HAC1* mRNA with the Ire1 RNase domain, which is mediated by the 3'-BE containing a conserved element (5'-$G_{1143}GCGC_{1147}$-3') (14). Our data implicated the kinase activity of Kin1 and Kin2 in *HAC1* mRNA splicing and translation (14); however, the mechanism by which Kin1 and Kin2 controls these physiological processes has not been clearly defined. Because *cis*-acting regulatory elements located at the 3'-UTR of mRNAs can influence their localization by interacting with RNA binding proteins(41), it is tempting to speculate that Kin1 and Kin2 control the formation of an RNP complex on the 3'-BE or modulate an existing RNP complex that drives *HAC1* mRNA targeting, splicing and/or translation. identify the components of this RNP, we identified proteins that associated with a 3'-BE mini RNA (Fig 1B, Table 1), including Pal2 which is a putative *in vitro* substrate of Kin2 (26).

In addition to Pal2, the yeast genome also encodes a paralogous protein Pal1. The *pal1Δ pal2Δ* strain was sensitive to low-dose of tunicamycin on medium containing galactose (a

less preferred carbon and energy source compared to glucose). Tunicamycin inhibits the enzyme GlcNAc 1 (N-acetylglucosamine)-phosphotransferase that transfers of GlcNAc-P to from UDP-GlcNAc to dolichyl-phosphate, a step in the formation of N-linked glycosylation of nascent protein. Thus, the absence of exogenous glucose may limit the pool of GlcNAc available for protein N-linked glycosylation, sensitizing cells to ER stress. The mechanistic details of why galactose enhances the tunicamycin sensitivity of the *pal1Δ pal2Δ* double deletion strain require further investigation.

We observed a functional overlap between Pal1 and Pal2 paralogs, allowing them to compensate each other's loss in mediating ER stress response (Figs. 2A, 4A, 4C). We also observed that Kin2 uniquely phosphorylates Pal2 (Fig 6C, which appears to be functionally relevant in the regulation of ER protein homeostasis. Unique paralog-specific functions of Pal1 and Pal2 have been previously reported. Pal2 associates with the endocytic coat factors to promote clathrin-mediated endocytosis (42), whereas Pal1 plays a critical role in the formation of endocytic sites (31). Pal1 contributes to cell polarity both in budding and fission yeast, a process essential for differentiation, morphogenesis and migration (43). Like budding yeast, the Pal1 ortholog in the fission yeast *S. pombe* plays an important role in maintaining cell morphology (44).

The functional divergence between Pal1 and Pal2 can be attributed in part to differences in their primary sequence and patterns of expression. For instance, *PAL2* mRNA, but not *PAL1* mRNA, contains an intron sequence. Pal1 and Pal2 have only 45% sequence identity at the protein level (fig S2). Moreover, only Pal2 harbors a consensus phosphorylation site sequence for Kin1 and Kin2, which is located within a cluster of phosphorylation sites that collectively are essential for its function in the UPR. Divergent phosphorylation is a well-established mechanism for differential regulation of paralogous proteins, which in some cases involves the acquisition of distinct kinase consensus sequences(45,46). Our data suggest that both Pal1 and Pal2 are low abundance proteins and are almost undetectable by Western blot analysis (Fig 4C). However, deletion of the N-terminal variable region makes both proteins stable. CD spectra suggests that Pal2 is likely a disordered protein (Fig 6A) and likely stabilized by its partner proteins to be able to function as a protein with pleotropic actions. More detailed functional analyses of Pal1 and Pal2 are necessary to fully determine and how they buffer each other's function, how they have evolved in increasing the adaptability to changing environmental conditions, and how their paralog dependency is driven by post-translational regulation.

Both Pal1 and Pal2 proteins contain both conserved and unique phosphorylation sites (>50 in Pal1 and >20 in Pal2) with an overall 45% sequence identity (figs. S2 and S3). Kin2 specifically phosphorylated Pal2 on Ser^{222} in vitro (Fig 6C and fig S5C), but Pal1 (Fig 6D). A single mutation of Ser^{222} was not sufficient to reduce the ER stress response; however, mutations of four consecutive phosphorylated residues (Ser^{222}, Thr^{223}, Thr^{224}, and/or Thr^{225}) to non-phosphorylatable alanine reduced the ability of *pal1Δ pal2Δ* strain to mount ER stress responses (Fig 7A). These results demonstrate that phosphorylation of all four residues in Pal2 likely plays an important role in ER stress response. Kin1/2 appears to act redundantly with the other unidentified kinases to promote Pal2 function in the UPR, presumably to provide robustness to the system by allowing Pal2 to function under

conditions where specific kinases may be inactive. Further work will be required to identify these additional kinases that phosphorylate Pal2 and to understand the condition-specific contributions of Kin1/2 and other Pal2 kinases to the ER stress response. Together, these data identify a Kin2-Pal2 signaling pathway that contributes to *HAC1* mRNA processing.

Several lines of evidence show that mRNAs can be specifically targeted to distinct subcellular compartments, raising the possibility that they are locally translated de-repressed to facilitate interaction and enable crosstalk of their translational products to other cellular machineries (47). However, our understanding of how cells sort mRNAs to specific sites is still limited. mRNA localization signals are commonly found within their 3′-UTRs, as with the 3'-BE in the *HAC1* mRNA that mediates co-localization with Ire1 (7). This co-localization is evident in the formation of microscopic foci of *HAC1* mRNA under conditions of ER stress (7,14).

Kin2 has been localized to the cytoplasmic face of the plasma membrane(48), at sites of polarized growth(34), and at intracellular membranes (38). Pal2 is predominantly located near the cell membrane and inside the cytoplasm (42). Thus, it is likely that Pal2 can shuttle between the plasma membrane and cytoplasm, and the interaction of Pal2 with the *HAC1* 3'-BE is induced by ER stress, or alternatively the pre-existing RNA-protein complex is maintained as the *HAC1* mRNA is relocalized. We posit that Pal1 and Pal2 likely contribute to the fine-tuning of Ire1 and/or *HAC1* mRNA foci formation. However, it is still unclear how Pal1 and Pal2 participate in the formation of these foci. Further mechanistic details governing *HAC1* mRNA targeting will necessitate the identification of core 3'-BE-specific RNP components.

In summary, our work unravels a Kin1/2-regulatory network as critical features of dynamic UPR signaling networks. We propose a model for the integration of Kin- and Ire1-mediated UPR signaling pathways (Fig 8). During ER stress, both Ire1 and Kin are activated. Ire1 is activated by dimerization, oligomerization and auto-phosphorylation (32,49). Kin1/2 are activated when its kinase domain is released by an unknown mechanism from the KA1 domain, which may relieve autoinhibition, probably because the KA1 domain binds phospholipids through the same interface it uses for the intramolecular association with the catalytic domain. Subsequently, the Kin2 kinase domain is activated by phosphorylation of its activation loop residue (Thr^{302} in Kin2) in a *trans* mechanism (38). Active Kin and the unknown kinase phosphorylate Pal2 at multiple sites, thus likely facilitating the targeting of the translationally repressed *HAC1* mRNA to the active Ire1 to excise its intron. The translation of *HAC1* mRNA is then de-repressed, resulting in production of an active transcription factor.

MATERIALS AND METHODS

Yeast strains, growth and gene disruption.

Standard *S. cerevisiae* media was used to grow and analyze the yeast strains. To construct the *pal1Δ pal2Δ* strain, we first replaced the *KanMX* cassette in the *pal1::KanMX* strain with the *NatMX* gene by the standard PCR-mediated gene disruption protocol. In the resulting *pal1::NatMX* strain, the *PAL2 gene* was disrupted by *KanMX to* generate the double

deletion strain. To generate the *kin1Δ kin2Δ snf1Δ* strain we first disrupted the *KanMX* gene in the *snf1Δ* strain (*MATa his3-Δ1 leu2-Δ0 met5-Δ0 ura3Δ0 snf1::KanMX*, yeast deletion collection) with the hphMX4 cassette (to generate *MATa his3-Δ1 leu2-Δ0 met5-Δ0 ura3-Δ0 snf1::hphMX*). The genomic DNA of this strain (*snf1::hphMX*) was used as a template to amplify the hphMX cassette using primers annealing ~200-bases upstream and downstream of the *SNF1* open reading frame. The amplified PCR product was used to disrupt the *SNF1* gene in the *kin1Δ kin2Δ* strain (*MATa his3-Δ1 leu2-Δ0 met5-Δ0 ura3-Δ0 kin1::NatMX kin2::kanMX*). The list of yeast strains used in this study is shown in table S1.

Plasmids and Mutagenesis

Plasmids were generated using standard gene manipulation techniques. Mutations were generated by fusion PCR using standard protocols. The desired mutation in each plasmid was confirmed by sequencing followed by analysis using the SnapGene software (https://www.snapgene.com). The list of plasmids used in this study is shown in table S2.

Pull down of biotinylated RNA and protein

Yeast cells expressing the 3'-BE-RMB or 5'-RD-RMB were grown in SC-uracil medium until the OD_{600} reached 0.8. Then, 4-thiouracil (20 mM) and DTT (5 mM) were added and cells were grown for another 3 hours. The culture was then harvested and washed with 1X PBS (phosphate buffered saline). Cells were re-suspended in 1X PBS in a 15 cm petri dish and exposed to UV light inside a UV-Stratalinker-1800 (Stratagene), twice for 2.5 minutes each (auto-crosslink setting). Cells were pelleted by centrifugation at 4 °C and lysed in 20 mM Tris-HCl, pH 7.4, 1 mM EDTA, 50 mM LiCl, 1% β-mercaptoethanol, 1 mg/ml heparin, 0.5mM phenylmethyl-sulfonyl fluoride (PMSF), 10 mM vanadyl adenosine. The RMB-conjugated RNAs were immobilized on Streptavidin agarose and bound proteins were eluted by 2X SDS dye (100 mM Tris-HCl pH 6.8. 4% SDS, 0.2% bromophenol blue). A fraction of the RNA elution was separated on SDS-PAGE and another fraction was sent to the Center of Biotechnology (Madison, WI, USA) for LC-MS/MS to identify associated proteins.

Protein purification and kinase assays

The yeast strain expressing Flag-tagged Kin1 or Kin2 from a galactose-inducible promoter was grown in a complete medium containing 10% galactose and 2% raffinose for 24 hours and harvested. The recombinant Flag-Kin1 and Flag-Kin2 proteins were purified using anti-FLAG M2 agarose (Sigma) using standard protocols. For protein expression in bacteria, we used BL21(DE3) cells and purified proteins by nickel agarose or glutathione cross-linked agarose (Thermo Scientific) as described previously (36). Purified proteins were mixed with Pal2 in a reaction buffer (20 mM Tris-HCl pH8.0, 50mM KCl, 25 mM $MgCl_2$ and 1mM PMSF) containing $\gamma-^{32}$P-ATP or $\gamma-^{33}$P-ATP. The reaction mixture was quenched by addition of 2X SDS buffer and separated by an SDS-PAGE. The gel was stained, dried and subjected to autoradiography.

CD *spectroscopy*

Protein samples were analyzed at a concentration of 0.5 mg/mL in 20 mM sodium phosphate, pH 8.0. CD spectra were collected in 0.1 cm path length quartz cells on a Jasco

J-810 Spectropolarimeter. Spectra in the wavelength range of 190–360 nm were collected using the following acquisition parameters: 0.1 nm steps, 1 nm bandwidth, 4 s response, 100 millidegree sensitivity, and 50 nm/min scanning speed with an accumulation of 3. Secondary structure composition was estimated from the analysis of the CD spectrum by the BeStSel web server (51) (wavelength range used for analysis is 190–250 nm).

In vitro transcription, RNA isolation and reverse transcription (RT)-PCR

For *in vitro* transcription reactions, 200 ng DNA template (5'-GGGGCGTAATACGACTCACTATAGGGCGTGAGGTTGGCGCGCCCTCCTACAATTATTTGTGGCGACTGGGCAGCGACACTGAACA-3') was mixed with 1X T7 reaction buffer, 1mM rNTP mix, 1 U RNase-OUT and 1 U T7 RNA polymerase (NEB M0251S). Reactions were incubated at 37 °C for 2 hours and run on a 1.5% agarose gel to quantify the amount of RNA product.

Yeast cells were grown in YEPD, YEPG or SC (synthetic complete) medium without appropriate nutrients at 30°C to an OD_{600} of ~0.5 – 06. DTT (5 mM unless otherwise indicated) or tunicamycin (0.5 μg/ml unless otherwise indicated) was added to the medium to induce ER stress and cells were grown further for another 2 hours. Cells were harvested and total RNA was isolated using the RNeasy mini kit (Qiagen). Purified RNA was quantified using a Nanadrop spectrophotometer (ND-1000, Thermo Scientific). Purified RNA was used to synthesize first strand cDNA by a Superscript™-III reverse transcriptase (Invitrogen 18080–093) and a reverse primer (5′CCCACCAACAGCGATAATAACGAG-3′) that corresponded to nucleotides +1002 to 1025. To assay *HAC1* mRNA splicing, synthetic cDNA was PCR-amplified using a forward primer (5′-CGCAATCGAACTTGGCTATC CCTACC-3′) that corresponded to nucleotides +35 to 60 and a reverse primer (5′-CCCACCA ACAGCGATAATAACGAG-3′) that corresponded to nucleotides +1002 to 1025. The PCR-amplified products were then run on a 1.5% agarose gel to separate spliced ($HAC1^s$) and un-spliced ($HAC1^u$) forms of *HAC1* mRNA. Quantities of $HAC1^s$ and $HAC1^u$ were measured using ImageJ. Percent splicing was calculated as $Hac1^s$ / ($HAC1^s$ + $HAC1^u$)*100%.

Whole cell extract preparation and Western blot analysis

Yeast cells were grown in YEPD, YEPG or SC medium without appropriate nutrients until the OD_{600} reached 0.6. DTT (5 mM) or tunicamycin (0.5 μg/ml unless indicated otherwise) was added to the medium to induce ER stress, and cells were harvested after 2 hours. Whole cell extracts (WCEs) were prepared by the TCA method as described previously (52). Proteins were fractioned by SDS–PAGE and Western blot analysis was performed using rabbit anti-Hac1 (Thermo Fisher Scientific, USA), anti-FLAG-M2 mouse monoclonal (Sigma; Cat#F3165), or mouse anti-PGK1 (22C5D58) monoclonal (Invitrogen; Cat #459250) antibodies.

Phos-tag SDS-PAGE and Western blot analysis

Phos-tag gels were made with 8% running (resolving) gel and 4.5% stacking gel. The 8% resolving gel was prepared with a 8% acrylamide/bis-acrylamide solution (29:1), 375 mM Tris-HCl pH 8.8, 100 μM $MnCl_2$, 50 μM phos-tag, 0.1% SDS, 0.1% APS and 0.01%

TEMED. The 4.5% stacking gel was prepared with a 4.5% acrylamide/bis-acrylamide solution (29:1), 125 mM Tris-HCl pH 6.8, 0.1% SDS, 0.1% APS and 0.01% TEMED. Phos-tag gels were run in Tris-glycine buffer (25 mM Tris, 250 mM glycine and 0.1% SDS) at a constant 100 voltage. Separated proteins in the gel was transferred to nitrocellulose membrane overnight in Tris-glycine transfer buffer (25 mM Tris and 250 mM glycine). Blots were probed with anti-Flag antibody.

UPRE-driven LacZ reporter assay

Yeast cell was transformed with a *URA3* plasmid containing a *LacZ* reporter gene under the control of an UPR element (UPRE) of the yeast *KAR2* gene (53). Transformants were grown overnight, diluted to an OD_{600} ~0.2 in a synthetic complete (SC) medium without uracil and allowed to grow until the OD_{600} reached ~0.6 – 0.8. The culture was then split into two flasks: half of the culture was grown in the presence of 5mM DTT and the remainder was grown without DTT. Cells were harvested after 4 hours, protein extracts were prepared and β-galactosidase activities were determined as described previously (52).

Electrophoretic mobility shift assay (EMSA)

Purified proteins were mixed with fluorescein tagged *HAC1*-3'-BE RNA oligomer (Sigma-Aldrich) in binding buffer (13 mM Tris-HCl pH 7.0, 1.5 mM $MgCl_2$). Reaction mixtures were incubated at 30 °C for 45 minutes with intermittent tapping and were separated using a 12% TBE (Tris-borate-EDTA) gel, and RNA was visualized under UV light. Gels were also stained with Coomassie to detect protein.

Supplementary Material

Refer to Web version on PubMed Central for supplementary material.

ACKNOWLEDGMENTS:

We would like to thank G. Sabat and G. Barret-Wilt of the University of Wisconsin-Madison Biotechnology Center Mass Spectrometry Facility for performing proteomic analysis.

FUNDING:

This study is supported by NIH grants 1R01GM124183 to M.D. and R01GM105947 to B.E.T.

REFERENCES AND NOTES

1. Schroder M (2008) Endoplasmic reticulum stress responses. Cell Mol Life Sci 65, 862–894 [PubMed: 18038217]
2. Walter P, and Ron D (2011) The Unfolded Protein Response: From Stress Pathway to Homeostatic Regulation. Science 334, 1081–1086 [PubMed: 22116877]
3. Ron D, and Walter P (2007) Signal integration in the endoplasmic reticulum unfolded protein response. Nat Rev Mol Cell Bio 8, 519–529 [PubMed: 17565364]
4. Xu C, Bailly-Maitre B, and Reed JC (2005) Endoplasmic reticulum stress: cell life and death decisions. J Clin Invest 115, 2656–2664 [PubMed: 16200199]
5. Cox JS, and Walter P (1996) A novel mechanism for regulating activity of a transcription factor that controls the unfolded protein response. Cell 87, 391–404 [PubMed: 8898193]

6. Ruegsegger U, Leber JH, and Walter P (2001) Block of HAC1 mRNA translation by long-range base pairing is released by cytoplasmic splicing upon induction of the unfolded protein response. Cell 107, 103–114 [PubMed: 11595189]
7. Aragon T, van Anken E, Pincus D, Serafimova IM, Korennykh AV, Rubio CA, and Walter P (2009) Messenger RNA targeting to endoplasmic reticulum stress signalling sites. Nature 457, 736–740 [PubMed: 19079237]
8. Calfon M, Zeng H, Urano F, Till JH, Hubbard SR, Harding HP, Clark SG, and Ron D (2002) IRE1 couples endoplasmic reticulum load to secretory capacity by processing the XBP-1 mRNA. Nature 415, 92–96 [PubMed: 11780124]
9. Yanagitani K, Kimata Y, Kadokura H, and Kohno K (2011) Translational Pausing Ensures Membrane Targeting and Cytoplasmic Splicing of XBP1u mRNA. Science 331, 586–589 [PubMed: 21233347]
10. Uemura A, Oku M, Mori K, and Yoshida H (2009) Unconventional splicing of XBP1 mRNA occurs in the cytoplasm during the mammalian unfolded protein response. J Cell Sci 122, 2877–2886 [PubMed: 19622636]
11. Cox JS, Shamu CE, and Walter P (1993) Transcriptional Induction of Genes Encoding Endoplasmic-Reticulum Resident Proteins Requires a Transmembrane Protein-Kinase. Cell 73, 1197–1206 [PubMed: 8513503]
12. Wang XZ, Harding HP, Zhang Y, Jolicoeur EM, Kuroda M, and Ron D (1998) Cloning of mammalian Ire1 reveals diversity in the ER stress responses. EMBO J 17, 5708–5717 [PubMed: 9755171]
13. Tirasophon W, Welihinda AA, and Kaufman RJ (1998) A stress response pathway from the endoplasmic reticulum to the nucleus requires a novel bifunctional protein kinase/endoribonuclease (Ire1p) in mammalian cells. Genes Dev 12, 1812–1824 [PubMed: 9637683]
14. Anshu A, Mannan MA, Chakraborty A, Chakrabarti S, and Dey M (2015) A novel role for protein kinase Kin2 in regulating HAC1 mRNA translocation, splicing, and translation. Mol Cell Biol 35, 199–210 [PubMed: 25348718]
15. Tassan JP, and Le Goff X (2004) An overview of the KIN1/PAR-1/MARK kinase family. Biol Cell 96, 193–199 [PubMed: 15182702]
16. Drewes G, and Nurse P (2003) The protein kinase kin1, the fission yeast orthologue of mammalian MARK/PAR-1, localises to new cell ends after mitosis and is important for bipolar growth. FEBS Lett 554, 45–49 [PubMed: 14596912]
17. Bhalerao RP, Salchert K, Bako L, Okresz L, Szabados L, Muranaka T, Machida Y, Schell J, and Koncz C (1999) Regulatory interaction of PRL1 WD protein with Arabidopsis SNF1-like protein kinases. Proc Natl Acad Sci U S A 96, 5322–5327 [PubMed: 10220464]
18. Kemphues KJ, Priess JR, Morton DG, and Cheng NS (1988) Identification of genes required for cytoplasmic localization in early C. elegans embryos. Cell 52, 311–320 [PubMed: 3345562]
19. Drewes G, Ebneth A, Preuss U, Mandelkow EM, and Mandelkow E (1997) MARK, a novel family of protein kinases that phosphorylate microtubule-associated proteins and trigger microtubule disruption. Cell 89, 297–308 [PubMed: 9108484]
20. Wu Y, and Griffin EE (2017) Regulation of Cell Polarity by PAR-1/MARK Kinase. Curr Top Dev Biol 123, 365–397 [PubMed: 28236972]
21. Elbert M, Rossi G, and Brennwald P (2005) The yeast par-1 homologs kin1 and kin2 show genetic and physical interactions with components of the exocytic machinery. Mol Biol Cell 16, 532–549 [PubMed: 15563607]
22. Donovan M, Romano P, Tibbetts M, and Hammond CI (1994) Characterization of the KIN2 gene product in Saccharomyces cerevisiae and comparison between the kinase activities of p145KIN1 and p145KIN2. Yeast 10, 113–124 [PubMed: 8203145]
23. Lee ME, Rusin SF, Jenkins N, Kettenbach AN, and Moseley JB (2018) Mechanisms Connecting the Conserved Protein Kinases Ssp1, Kin1, and Pom1 in Fission Yeast Cell Polarity and Division. Curr Biol 28, 84–92 e84 [PubMed: 29249658]
24. Nishi Y, Rogers E, Robertson SM, and Lin R (2008) Polo kinases regulate C. elegans embryonic polarity via binding to DYRK2-primed MEX-5 and MEX-6. Development 135, 687–697 [PubMed: 18199581]

25. Drewes G, Trinczek B, Illenberger S, Biernat J, Schmitt-Ulms G, Meyer HE, Mandelkow EM, and Mandelkow E (1995) Microtubule-associated protein/microtubule affinity-regulating kinase (p110mark). A novel protein kinase that regulates tau-microtubule interactions and dynamic instability by phosphorylation at the Alzheimer-specific site serine 262. J Biol Chem 270, 7679–7688 [PubMed: 7706316]
26. Jeschke GR, Lou HJ, Weise K, Hammond CI, Demonch M, Brennwald P, and Turk BE (2018) Substrate priming enhances phosphorylation by the budding yeast kinases Kin1 and Kin2. J Biol Chem 293, 18353–18364 [PubMed: 30305396]
27. Vasudevan S, and Steitz JA (2007) AU-rich-element-mediated upregulation of translation by FXR1 and Argonaute 2. Cell 128, 1105–1118 [PubMed: 17382880]
28. Ruegsegger U, Leber JH, and Walter P (2001) Block of HAC1 mRNA translation by long-range base pairing is released by cytoplasmic splicing upon induction of the unfolded protein response. Cell 107, 103–114 [PubMed: 11595189]
29. Castello A, Fischer B, Eichelbaum K, Horos R, Beckmann BM, Strein C, Davey NE, Humphreys DT, Preiss T, Steinmetz LM, Krijgsveld J, and Hentze MW (2012) Insights into RNA biology from an atlas of mammalian mRNA-binding proteins. Cell 149, 1393–1406 [PubMed: 22658674]
30. Tsvetanova NG, Riordan DP, and Brown PO (2012) The yeast Rab GTPase Ypt1 modulates unfolded protein response dynamics by regulating the stability of HAC1 RNA. PLoS Genet 8, e1002862 [PubMed: 22844259]
31. Carroll SY, Stimpson HE, Weinberg J, Toret CP, Sun Y, and Drubin DG (2012) Analysis of yeast endocytic site formation and maturation through a regulatory transition point. Mol Biol Cell 23, 657–668 [PubMed: 22190733]
32. Lee KP, Dey M, Neculai D, Cao C, Dever TE, and Sicheri F (2008) Structure of the dual enzyme Ire1 reveals the basis for catalysis and regulation in nonconventional RNA splicing. Cell 132, 89–100 [PubMed: 18191223]
33. Hinnebusch AG (2011) Molecular Mechanism of Scanning and Start Codon Selection in Eukaryotes. Microbiol Mol Biol R 75, 434–467
34. Yuan SM, Nie WC, He F, Jia ZW, and Gao XD (2016) Kin2, the Budding Yeast Ortholog of Animal MARK/PAR-1 Kinases, Localizes to the Sites of Polarized Growth and May Regulate Septin Organization and the Cell Wall. PLoS One 11, e0153992 [PubMed: 27096577]
35. Gelperin DM, White MA, Wilkinson ML, Kon Y, Kung LA, Wise KJ, Lopez-Hoyo N, Jiang L, Piccirillo S, Yu H, Gerstein M, Dumont ME, Phizicky EM, Snyder M, and Grayhack EJ (2005) Biochemical and genetic analysis of the yeast proteome with a movable ORF collection. Genes Dev 19, 2816–2826 [PubMed: 16322557]
36. Dey M, Cao C, Dar AC, Tamura T, Ozato K, Sicheri F, and Dever TE (2005) Mechanistic link between PKR dimerization, autophosphorylation, and eIF2alpha substrate recognition. Cell 122, 901–913 [PubMed: 16179259]
37. Swaney DL, Beltrao P, Starita L, Guo A, Rush J, Fields S, Krogan NJ, and Villen J (2013) Global analysis of phosphorylation and ubiquitylation cross-talk in protein degradation. Nat Methods 10, 676–682 [PubMed: 23749301]
38. Ghosh C, Sathe L, Paprocki JD, Raicu V, and Dey M (2018) Adaptation to Endoplasmic Reticulum Stress Requires Transphosphorylation within the Activation Loop of Protein Kinases Kin1 and Kin2, Orthologs of Human Microtubule Affinity-Regulating Kinase. Mol Cell Biol 38
39. Mok J, Kim PM, Lam HY, Piccirillo S, Zhou X, Jeschke GR, Sheridan DL, Parker SA, Desai V, Jwa M, Cameroni E, Niu H, Good M, Remenyi A, Ma JL, Sheu YJ, Sassi HE, Sopko R, Chan CS, De Virgilio C, Hollingsworth NM, Lim WA, Stern DF, Stillman B, Andrews BJ, Gerstein MB, Snyder M, and Turk BE (2010) Deciphering protein kinase specificity through large-scale analysis of yeast phosphorylation site motifs. Sci Signal 3, ra12 [PubMed: 20159853]
40. Sathe L, Bolinger C, Mannan MA, Dever TE, and Dey M (2015) Evidence That Base-pairing Interaction between Intron and mRNA Leader Sequences Inhibits Initiation of HAC1 mRNA Translation in Yeast. J Biol Chem 290, 21821–21832 [PubMed: 26175153]
41. Andreassi C, and Riccio A (2009) To localize or not to localize: mRNA fate is in 3'UTR ends. Trends Cell Biol 19, 465–474 [PubMed: 19716303]

42. Moorthy BT, Sharma A, Boettner DR, Wilson TE, and Lemmon SK (2019) Identification of Suppressor of Clathrin Deficiency-1 (SCD1) and Its Connection to Clathrin-Mediated Endocytosis in Saccharomyces cerevisiae. G3 (Bethesda) 9, 867–877 [PubMed: 30679249]
43. Campanale JP, Sun TY, and Montell DJ (2017) Development and dynamics of cell polarity at a glance. J Cell Sci 130, 1201–1207 [PubMed: 28365593]
44. Ge W, Chew TG, Wachtler V, Naqvi SN, and Balasubramanian MK (2005) The novel fission yeast protein Pal1p interacts with Hip1-related Sla2p/End4p and is involved in cellular morphogenesis. Mol Biol Cell 16, 4124–4138 [PubMed: 15975911]
45. Lee YJ, Jeschke GR, Roelants FM, Thorner J, and Turk BE (2012) Reciprocal phosphorylation of yeast glycerol-3-phosphate dehydrogenases in adaptation to distinct types of stress. Mol Cell Biol 32, 4705–4717 [PubMed: 22988299]
46. Miller CJ, and Turk BE (2018) Homing in: Mechanisms of Substrate Targeting by Protein Kinases. Trends Biochem Sci 43, 380–394 [PubMed: 29544874]
47. Martin KC, and Ephrussi A (2009) mRNA localization: gene expression in the spatial dimension. Cell 136, 719–730 [PubMed: 19239891]
48. Tibbetts M, Donovan M, Roe S, Stiltner AM, and Hammond CI (1994) KIN1 and KIN2 protein kinases localize to the cytoplasmic face of the yeast plasma membrane. Exp Cell Res 213, 93–99 [PubMed: 8020610]
49. Korennykh AV, Egea PF, Korostelev AA, Finer-Moore J, Zhang C, Shokat KM, Stroud RM, and Walter P (2009) The unfolded protein response signals through high-order assembly of Ire1. Nature 457, 687–693 [PubMed: 19079236]
50. Moravcevic K, Mendrola JM, Schmitz KR, Wang YH, Slochower D, Janmey PA, and Lemmon MA (2010) Kinase associated-1 domains drive MARK/PAR1 kinases to membrane targets by binding acidic phospholipids. Cell 143, 966–977 [PubMed: 21145462]
51. Micsonai A, Wien F, Bulyaki E, Kun J, Moussong E, Lee YH, Goto Y, Refregiers M, and Kardos J (2018) BeStSel: a web server for accurate protein secondary structure prediction and fold recognition from the circular dichroism spectra. Nucleic Acids Res 46, W315–W322 [PubMed: 29893907]
52. Mannan MA, Shadrick WR, Biener G, Shin BS, Anshu A, Raicu V, Frick DN, and Dey M (2013) An ire1-phk1 chimera reveals a dispensable role of autokinase activity in endoplasmic reticulum stress response. J Mol Biol 425, 2083–2099 [PubMed: 23541589]
53. Normington K, Kohno K, Kozutsumi Y, Gething MJ, and Sambrook J (1989) S. cerevisiae encodes an essential protein homologous in sequence and function to mammalian BiP. Cell 57, 1223–1236 [PubMed: 2661019]

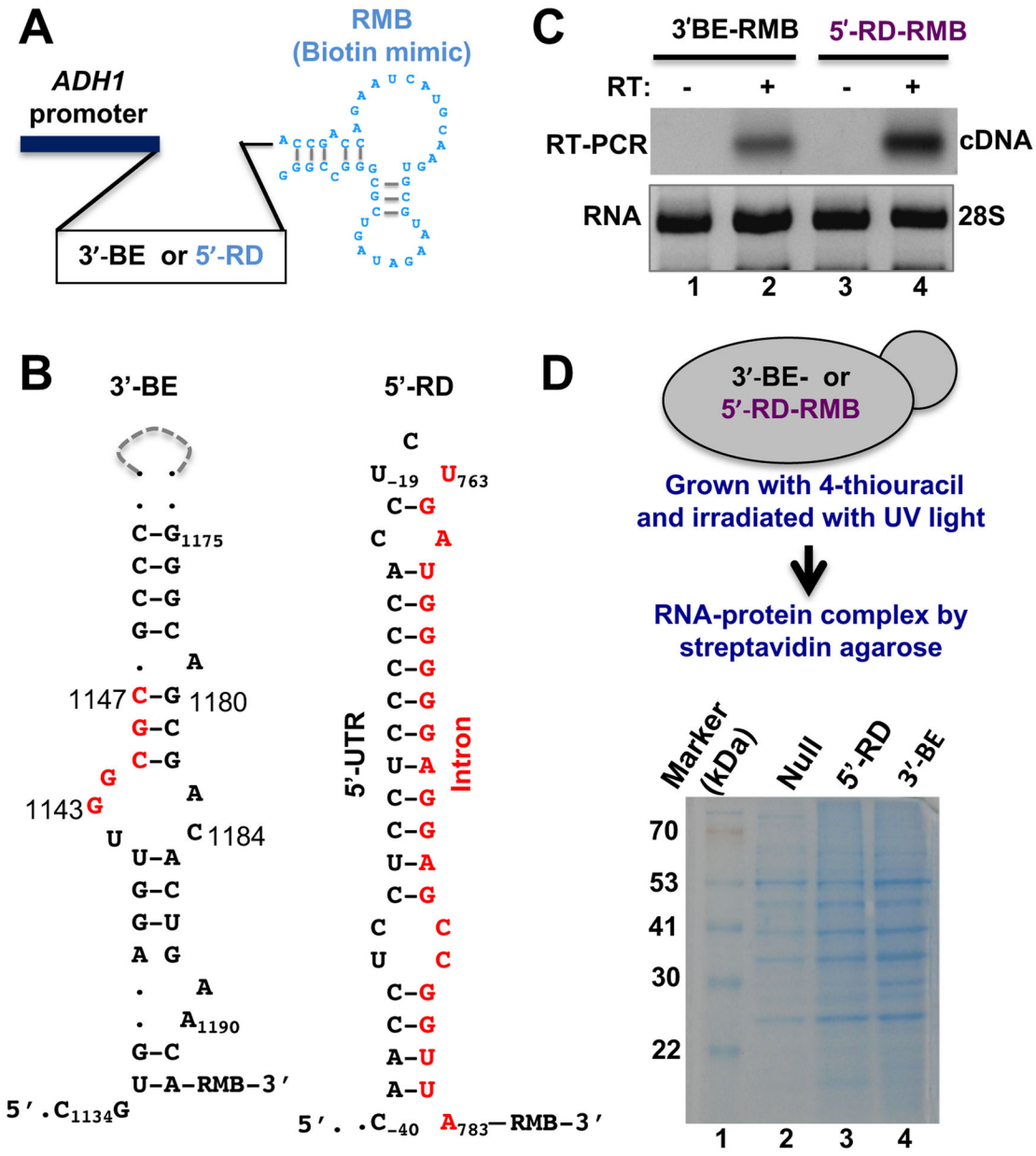

Figure 1: Analysis of proteins binding to the 3’-BE in *HAC1* mRNA.

(A) The template DNA sequence of the 3’-BE- or 5’-RD RNA was placed under the control of the constitutive *ADH1* promoter. The predicted structure of the RMB is shown.

(B) The predicted secondary structure of 3’-BE and 5’-RD RNAs is shown. The conserved RNA motif within the 3’-BE is shown in red. The 5’-RD consisting of 5’-UTR and intron are shown in black and red, respectively. The numbers indicate the nucleotide positions.

(C) To analyze mini RNA expression, cDNA was synthesized from total RNA isolated from yeast cells expressing the 3’-BE- and 5’-RD-RMB mini RNA constructs using gene-specific primers in the presence and absence of reverse transcriptase (RT). Representative of 2 independent experiments.

(D) Proteins bound to the 3’-BE- or 5’-RD-RMB mini RNA were electrophoresed and stained. Representative of 1 experiment.

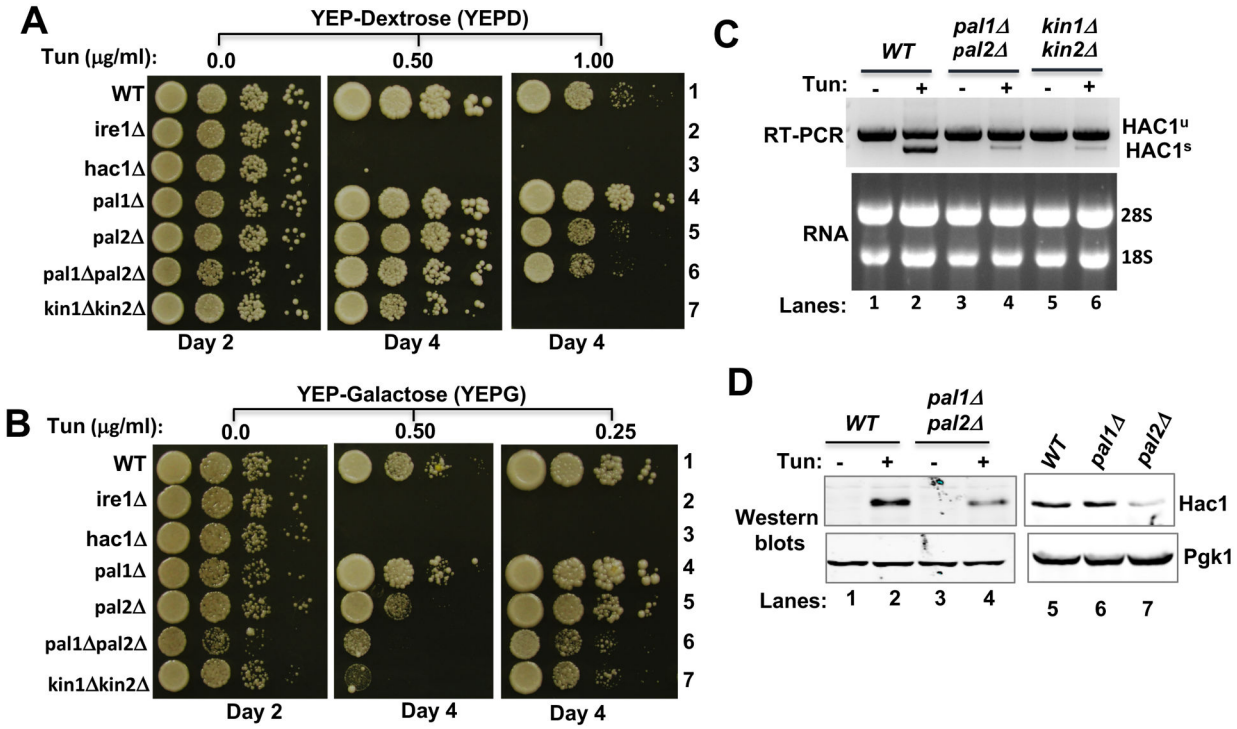

Figure 2: The *pal1*Δ *pal2*Δ strain is deficient in ER stress responses.

(A) & (B) The indicated yeast strains were grown, serially diluted and spotted on YEPD (A) or YEPG (B) solid medium containing the indicated concentrations of tunicamycin. Representative of 2 independent experiments.

(C) The indicated yeast strains were grown in YEPG medium with or without tunicamycin (Tun). cDNA was prepared from total RNA (lower panel) and the spliced ($HAC1^s$) and un-spliced ($HAC1^u$) forms of *HAC1* mRNA were detected. Representative of 2 independent experiments.

(D) The indicated yeast strains were grown in YEPG medium with or without tunicamycin (Tun). Whole cell extracts (WCEs) were isolated and subjected to Western blot analysis using antibodies to detect Hac1 and Pgk1. Representative of 2 independent experiments.

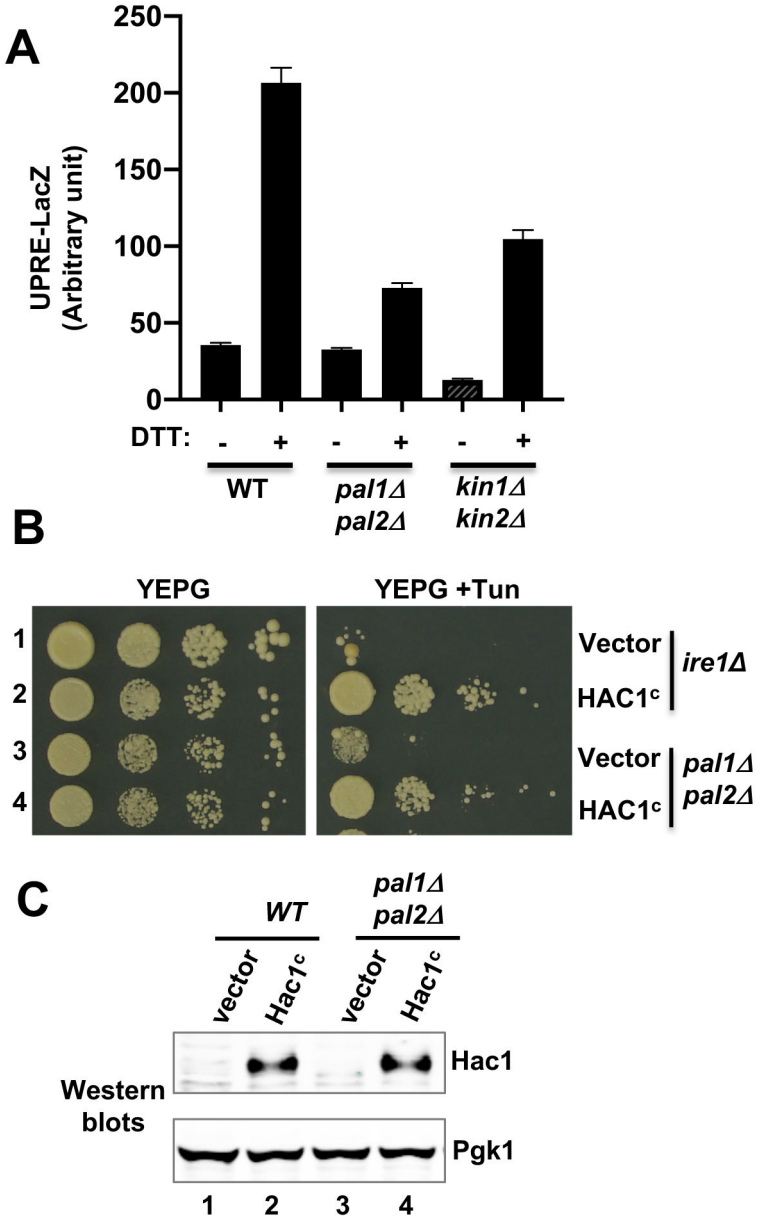

Figure 3: Analysis of Hac1 protein expression from the intron-less *HAC1* mRNA.

(A) Yeast strains (WT, *kin1Δkin2Δ* or *pal1Δpal2Δ*) transformed with a plasmid carrying the *UPRE*-driven LacZ reporter gene were grown in the presence (+) and absence (–) of DTT. β-galactosidase activity was measured in WCEs. Representative of 3 independent experiments.

(B) The indicated yeast strains expressing vector plasmid or the same vector containing an intron-less *HAC1* gene ($HAC1^c$) were grown serially diluted and spotted on YEPG medium with or without tunicamycin. Representative of 2 independent experiments.

(C) The same yeast strains as in (B) were grown in YEPG medium and whole cell extracts were isolated and subjected to Western blot analysis using antibodies to detect Hac1 and Pgk1. Representative of 2 independent experiments.

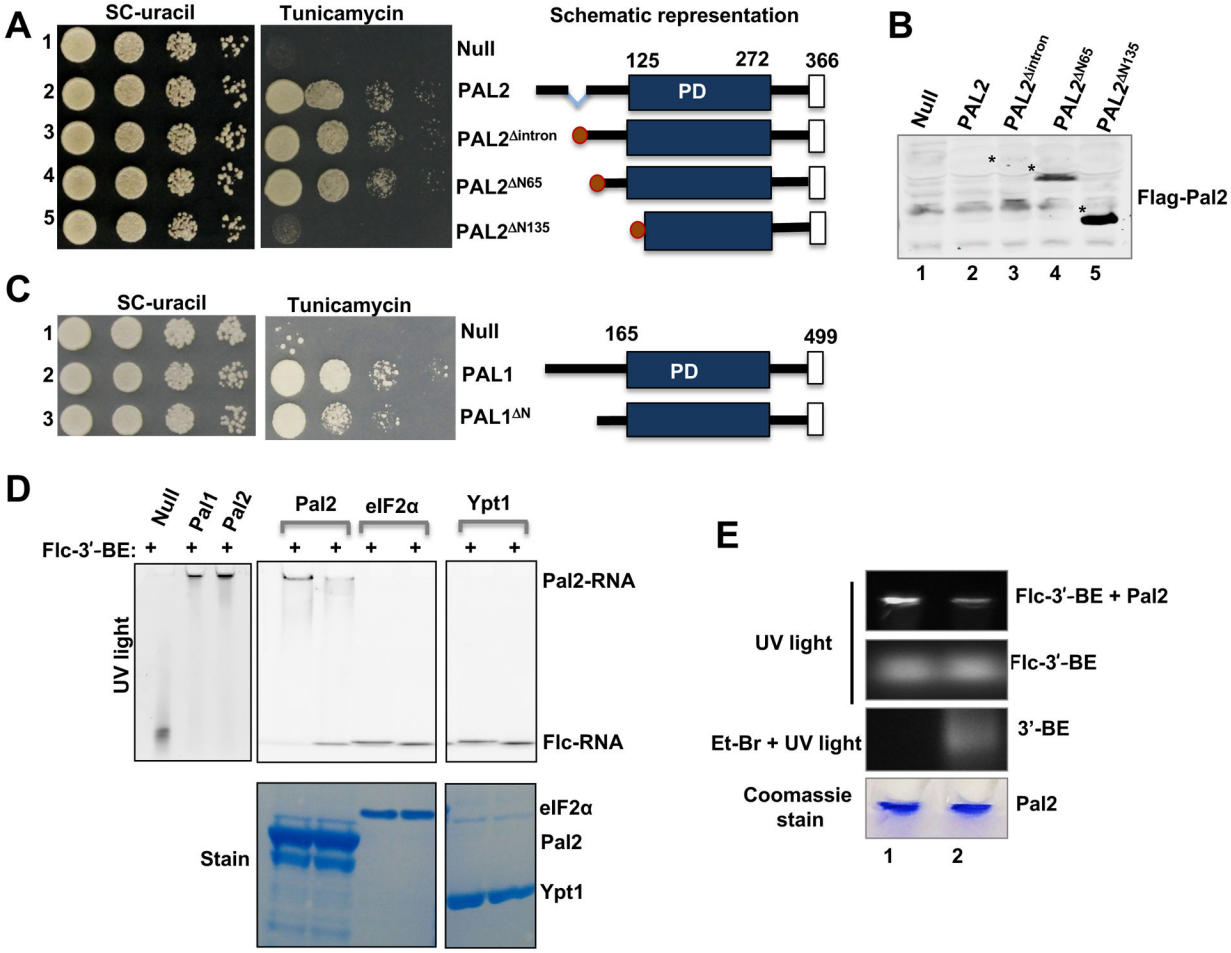

Figure 4: Pal1 and Pal2 are associated with *HAC1* mRNA

(A) The *pal1Δpal2Δ* strains expressing WT or mutant Pal2 were tested for growth on the complete synthetic (SC) medium without uracil or the same medium containing tunicamycin. Representative of 2 independent experiments. The right panel shows the schematic representations of WT and Flag-tagged (red circle) Pal2 constructs. The intronic region of the WT *PAL2* is colored light blue. The regions encoding the homologous Pal1 domains (PD, residues 125 to 272) are indicated by dark blue boxes.

(B) WCEs were prepared from the same yeast strains as in (A) and subjected to Western blot analysis to detect Flag. "*" indicates Pal2. Representative of 2 independent experiments.

(C) The *pal1Δpal2Δ* strains expressing WT Pal2 or its derivatives were tested for growth on the complete synthetic (SC) medium without uracil (Ura) or the same medium containing tunicamycin. Representative of 2 independent experiments. The right panel shows the schematic representations of WT and mutant Pal1 constructs.

(D) Electrophoretic mobility shift assay (EMSA) using a fluorescein-tagged synthetic RNA corresponding to the 3'-BE (Flc-3'-BE) and recombinant His_6-Pal1, His_6-Pal2, His_6-eIF2α or His_6-Ypt1. The reaction mixture was resolved with native gels and illuminated with ultraviolet (UV)-light to see the RNA-protein interaction. Representative of 2 independent experiments.

(E) Flc-3'-BE (2nd panel) was mixed with the recombinant His_6-Pal2 protein (bottom panel) in a binding buffer with (lane 2) or without (lane 1) the non-fluorescent 3'-BE (3rd panel). The reaction mixture was resolved with native gels and illuminated with ultraviolet (UV)-light to see the Flc-3'-BE•Pal2 interaction. The portion of gel showing the Flc-3'-BE bound to Pal2 is shown (top panel). Representative of 2 independent experiments.

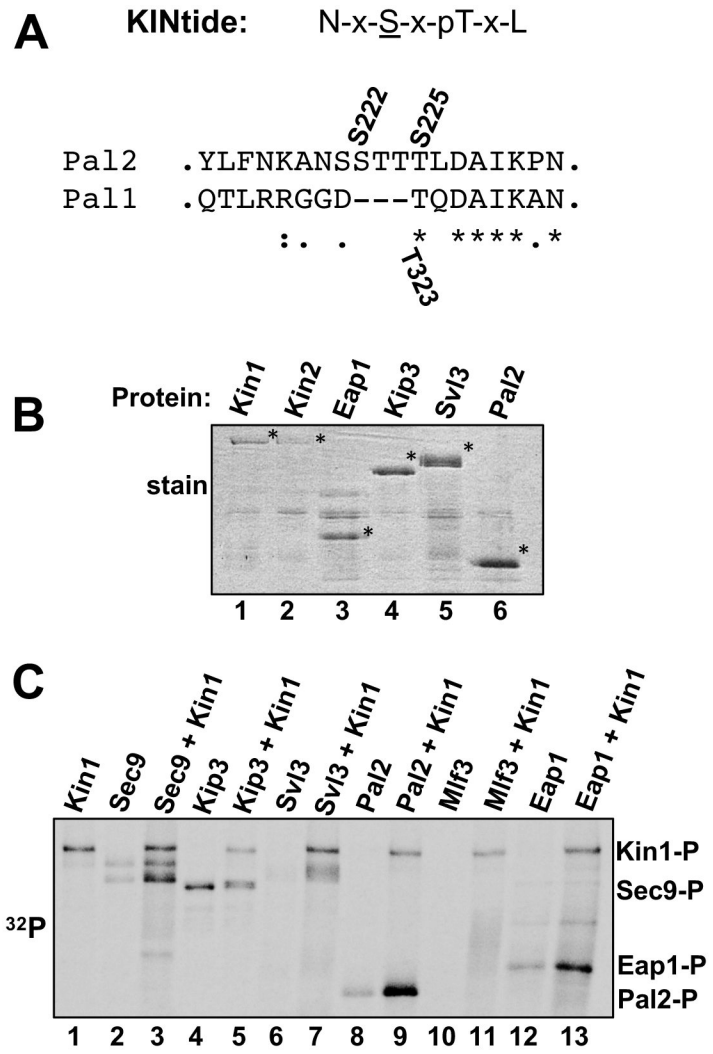

Figure 5: Kin1 phosphorylates Pal2 *in vitro*

(A) The consensus sequence for Kin phosphorylation and the corresponding sequences in Pal1 and Pal2. x indicates any amino acid and pT indicates phospho-threonine.

(B) The indicated proteins were purified from yeast and subjected to SDS-PAGE analysis. "*" denotes the protein of interest. Representative of 2 independent experiments.

(C) Purified proteins were mixed with Kin1 in a reaction mixture containing radiolabeled ATP (γ–^{33}P-ATP) and separated by SDS-PAGE. Radiolabel incorporation was detected by autoradiograph. Representative of 2 independent experiments.

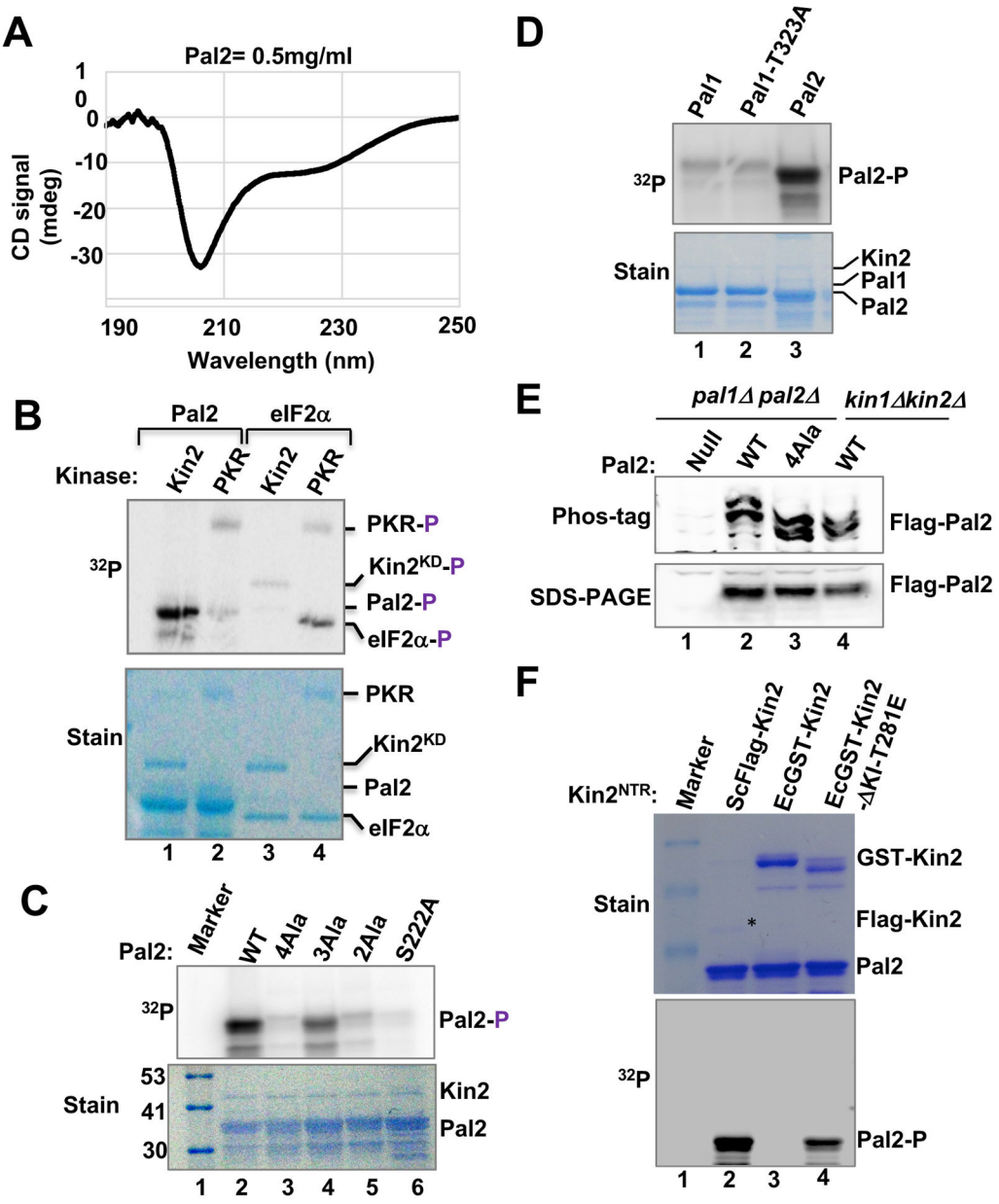

Figure 6: Kin2 phosphorylates the residue Ser-222 of Pal2 *in vitro*

(A) Circular dichroism (CD) spectra of recombinant Pal2 (0.5 mg/mL) was collected in the wavelength range of 190–360 nm. Representative of 2 independent experiments.

(B) Recombinant His_6-Pal2 (residues 65–366) or eIF2α protein was incubated with purified Kin2 or PKR in a kinase reaction containing γ-^{32}P-ATP and resolved by SDS-PAGE. Gel was stained with Coomassie blue (lower panel) and subjected to autoradiography (upper panel). Representative of 2 independent experiments.

(C) Recombinant His_6-Pal2 (residues 65–366) and the indicated mutants were subjected to kinase assay. Pal2-4Ala = S222A,T223A,T224A and T225A. Pal2-3Ala = T223A,T224A and T225A. Pal2-2Ala = S222A and T224A. Protein markers (kDa) are indicated. Representative of 2 independent experiments.

(D) Recombinant His_6-Pal1 (residues 165–499) protein was subjected to kinase assay with purified Kin2 and $\gamma-^{33}$P-ATP as described in (B). Representative of 2 independent experiments.

(E) WCEs were prepared from the indicated yeast strains containing a vector plasmid (null) or the same plasmid containing the Flag-tagged WT or 4Ala mutant Pal2. WCEs were subjected to normal SDS-PAGE or Phos-tag SDS-PAGE gel followed by Western blot analysis to detect Flag. Representative of 3 independent experiments.

(F) Recombinant His_6-Pal2 (residues 65–366) was subjected to kinase assay with Flag-tagged Kin2 purified from yeast (ScFlag-Kin2), GST-Kin2 purified fom *E. coli* (EcGST-Kin2) or GST-Kin2-T281E purified fom *E. coli* (EcGST-Kin2-T281E) as described in (B). Representative of 2 independent experiments.

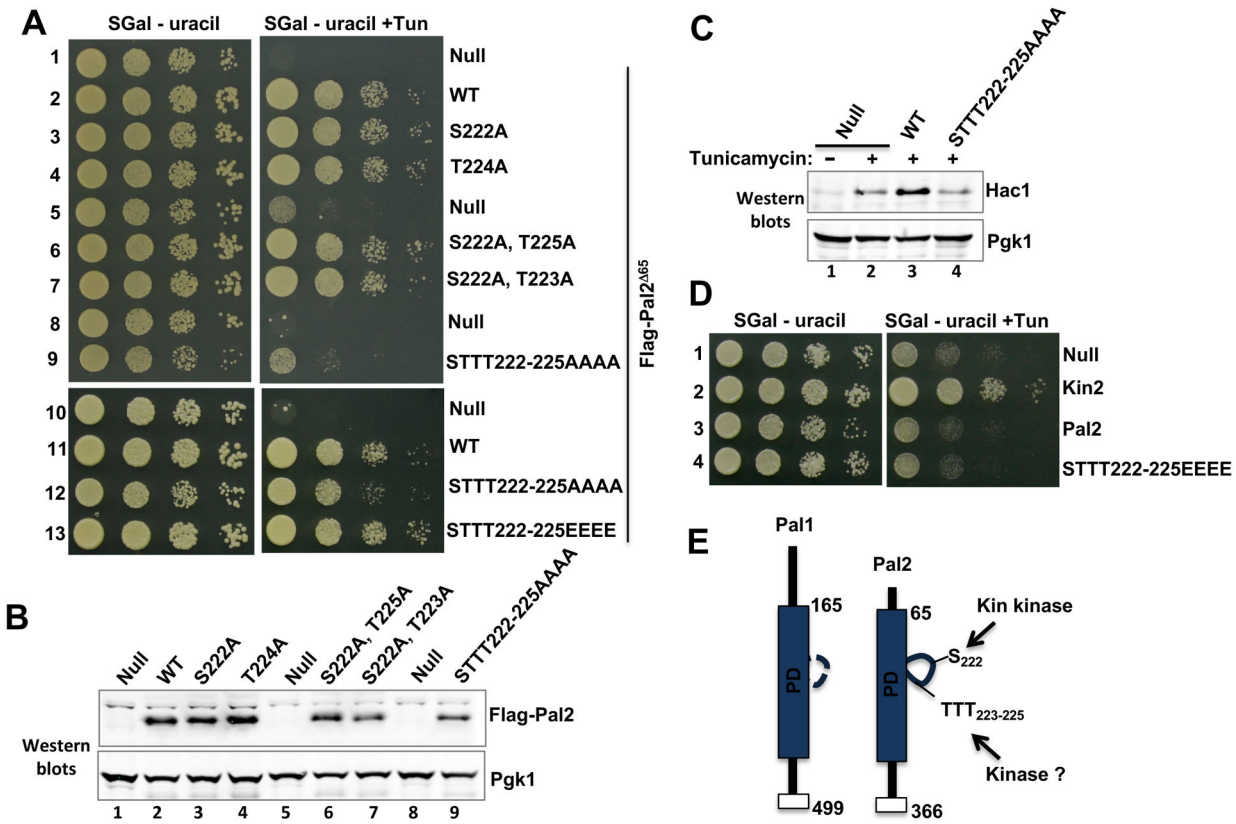

Figure 7: Phosphorylation of Pal2 is important for ER stress responses

(A) The *pal1Δ pal2Δ* strains expressing WT or mutant Pal2 were tested for growth on synthetic complete medium with and without tunicamycin. Representative of 3 independent experiments.

(B) WCEs from the same strains as in (A) were subjected to Western blot analysis to detect Flag. Representative of 2 independent experiments.

(C) The selected *pal1Δ pal2Δ* yeast strains as in (A) were grown in synthetic complete medium without uracil in the presence (+) or absence (–) of tunicamycin and WCEs were subjected to Western blot analysis for Hac1 and Pgk1. Representative of 2 independent experiments.

(D) The *kin1Δ kin2Δ* strains expressing WT Kin2, WT Pal2 or Pal2$^{\Delta N65}$-STTT222–225EEEE (STTT222–225EEEE) were tested for growth on synthetic complete medium with and without tunicamycin. Representative of 2 independent experiments.

(E) The homologous Pal1 domains (PD) in Pal1 and Pal2 are indicated by dark blue boxes. The phosphorylation loop of Pal2 is shown.

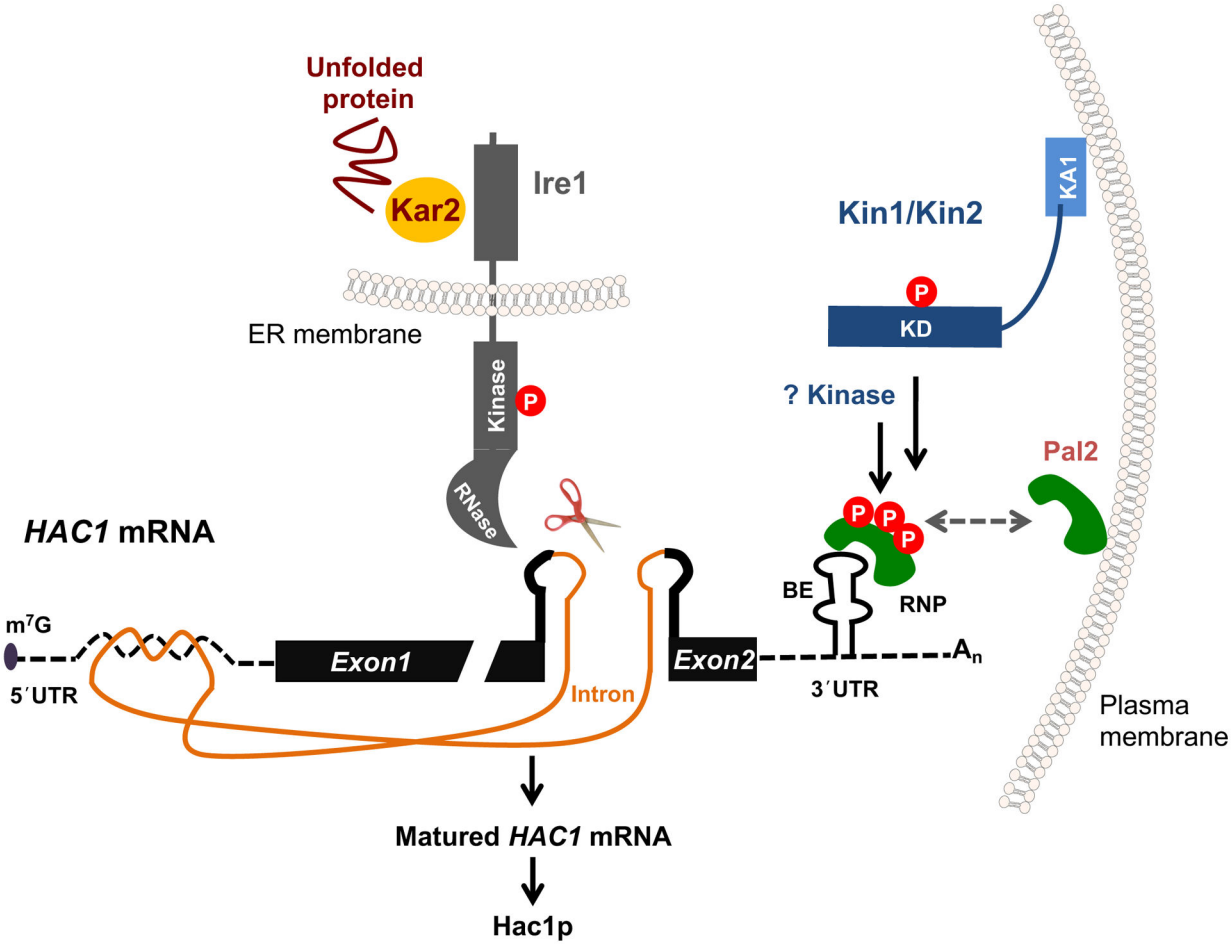

Figure 8: Proposed role of Pal2 in the Ire1-*HAC1* mediated UPR.

The ER-resident chaperone Kar2 binds to the lumenal domain of Ire1 and keeps it in an inactive form. During the ER stress, unfolded proteins (scribbled red line) accumulate inside the ER lumen and titrate Kar2, thus activating the cytoplasmic kinase and RNase domain of Ire1. The active RNase domain cleaves the intron from the *HAC1* mRNA. The exons (grey bars) of *HAC1* mRNA are separated by an intron (orange dashed line) that interacts with the 5'-UTR (solid black) line of mRNA to form an inhibitory RNA duplex (RD). The KA1 domain (light blue bar) binds to the KD (dark blue bar) of Kin1 or Kin2, thus keeping the KD in an inactive form. Under stress conditions, the KD is activated by phosphorylation ("P" in a red circle) within the activation loop on residue Thr^{281} in a trans mechanism. The active KD then phosphorylates Pal2, which is likely associated with the 3'-BE and 3'-BE-specific RNP, thus targeting *HAC1* mRNA to the ER stress site.

Table 1:

A list of putative 3’-BE and 5’-RD-specific proteins

	Function	**Protein**
3’BE-specific proteins	Metabolic enzymes	Leu2, NTH1, FAA4, Frs1, PNC1, Ams1, Prs5, Cab3, Apa1, Pgm1,
	Transporter	Vma8
	Transcription	Rpb2, Pbp4
	Endocytosis	Pan1
	Translational repressor	Ssd1
	mRNA export	Arx1
	mRNA localization	She3
	P-body	Xrn1
	Kinases	Cdc28, Bcy1, Ypk1
	Cytokinesis	Shs1, Cdc3, Vrp1
	Unknown	Pal2
5’RD-specific proteins	Metabolic enzymes	Mmf1, Snz1, NCE103, Arg5, Bna1, Sry1, TPl1, Adk1, Met10, Cys3, Ade17, Sfa1, Spe3,
	Transporter	Oac1, Pho88
	Chaperone	Phb2, Mge1, Ggc1
	V-ATPase	Vma10
	Phosphatase	Sac1
	Translocase	Tom70
	Unknown	Aim46